

I N S T I T U T D E S T A T I S T I Q U E
B I O S T A T I S T I Q U E E T
S C I E N C E S A C T U A R I E L L E S
(I S B A)

UNIVERSITÉ CATHOLIQUE DE LOUVAIN



D I S C U S S I O N
P A P E R

2011/13

**MULTIVARIATE VOLATILITY MODELING
OF ELECTRICITY FUTURES**

BAUWENS, L., HAFNER, C. and D. PIERRET

CORE DISCUSSION PAPER

2011/11

MULTIVARIATE VOLATILITY MODELING OF ELECTRICITY FUTURES

Luc Bauwens¹, Christian Hafner^{2*}, and Diane Pierret³

April 21, 2011

Abstract: We model the dynamic volatility and correlation structure of electricity futures series of the European Energy Exchange index, using an asymmetric GARCH model for volatilities and augmented dynamic conditional correlation (DCC) models for correlations. In particular, we allow for smooth changes in the unconditional volatilities and correlations through a multiplicative component that we estimate nonparametrically. We also introduce exogenous variables in our new multiplicative DCC model to account for congestion and seasonality in short-term conditional volatilities. We find different correlation dynamics for long and short-term contracts and the new model achieves higher forecasting performance compared to a standard DCC model.

Keywords: dynamic conditional correlation, electricity futures, forecasting.

JEL Classification: C32, C53, C58.

*Correspondence to: Christian Hafner, ISBA, 20 Voie du Roman Pays, B-1348 Louvain-La-Neuve, Belgium.
Tel.: +32 10 47 43 06; fax: +32 10 47 30 32; e-mail: christian.hafner@uclouvain.be

¹Université catholique de Louvain, CORE.

²Université catholique de Louvain, ISBA and CORE.

³Université catholique de Louvain, ISBA.

The authors would like to thank Niels Haldrup and Almut Veraart, participants of the econometrics seminar at CREATES (University of Aarhus), the participants of the econometrics meeting of the Verein für Socialpolitik and the participants of the 4th international conference on Computational and Financial Econometrics (CFE'10) for their questions and useful comments.

This research was supported by the contract "Projet d'Actions de Recherche Concertées" 07/12-002 of the "Communauté française de Belgique", granted by the "Académie universitaire Louvain". This text presents research results of the Belgian Program on Interuniversity Poles of Attraction (IAP nr. P6/03) initiated by the Belgian State, Prime Minister's Office, Science Policy Programming.

1 Introduction

The econometric literature on electricity markets has mainly focused on analyzing and modeling the behavior of spot prices. For example, Carnero et al. (2007) use fractional integration to capture the long memory nature of electricity spot prices. Haldrup and Nielsen (2006) suggest a Markov regime-switching model with three regimes to reflect directional congestion. De Jong and Schneider (2009) analyze cointegration between gas and power spot prices. Bosco et al. (2010) analyze the interdependences between power spot prices of six European markets.

However, due to the intrinsic nature of electricity - non-storability, transmission constraints, seasonality and weather dependence, power stack function - futures represent a larger market than spot trading. Energy risk management uses futures to hedge against spot price risk but futures are also a substitute to spot trading for investors willing to take positions in power markets without the underlying physical constraints. The behavior of power prices is very specific and the absence of an empirical relationship between spot and futures time series motivates a separate model for forecasting futures prices.

In this paper, we are interested in understanding the volatility and the correlation structure of three futures contracts corresponding to different maturities. Recent developments in the domain of GARCH models deal with changes in levels of volatilities and correlations, either through regime shifts or through smooth evolutions. Engle and Rangel (2008) decompose the variance of returns into low-frequency and high-frequency components where the low-frequency component is approximated by spline functions and the high frequency component is a GARCH process. The factor-spline GARCH-DCC model of Rangel and Engle (2009) is a multivariate extension that allows conditional correlations to mean revert toward a slowly changing function within a factor asset pricing framework. In the multivariate multiplicative volatility model of Hafner and Linton (2010) the covariance matrix is decomposed into unconditional and conditional components where the unconditional component is estimated nonparametrically and the conditional component is a BEKK process. We propose a new multivariate volatility model that allows for smooth changes in the unconditional volatilities and correlations. The unconditional covariance matrix is specified nonparametrically as a smooth function of time and is estimated using a kernel estimator, while the conditional component is specified as a DCC process. The proposed model can be viewed as an extension of the multiplicative model of Hafner and Linton (2010) to the DCC case. We show that this extended version of the DCC model is not subject to the inconsistency problem revealed by Aielli (2009) for the standard DCC model of Engle (2002).

The multiplicative DCC model is applied to a set of futures contracts written on the index of the European Energy Exchange (EEX). We show that the evolution of the nonparametric unconditional covariance coincides with long-term trends in the power sector. The standardization of returns with this unconditional component allows identifying new variables exclusively affecting short term movements in conditional volatilities and correlations. Inspired by the model of Haldrup and Nielsen

(2006), we adapt a congestion model to account for transmission shocks in the volatility of electricity futures. Our congestion model for volatilities also accounts for the seasonality attached to the delivery date of short-term contracts. More flexibility in the modeling of conditional correlations is reached with the generalized DCC model of Hafner and Franses (2009). We also show that the forecasting performance is improved compared to the conditional correlation model that ignores long-term trends.

The paper is structured as follows: in Section two, we provide a description of electricity markets with the example of the EEX market. In Section three, we present the data of EEX futures prices that we use and a vector-error correction model that serves to filter the series for their co-movements in means. In Section four, the results of standard DCC estimation are discussed. In Section five, our new multiplicative DCC model is introduced. We apply this model to EEX futures in Section six. In the next section, we discuss the forecasting performance of the new model compared to the standard DCC process, and in the last section we conclude.

2 Electricity markets: the EEX case

The oldest electricity wholesale trading market is the Scandinavian Nord Pool market that was the first to introduce electricity futures contracts (Borovkova and Geman (2006)). Most papers dealing with electricity prices are referring to Nord Pool prices because of the exemplary efficiency of the market and the availability of price series over long time horizons. Besides, the European Energy Exchange (EEX) has recently become the leading energy exchange in continental Europe in terms of sales and number of trading participants (see www.eex.com). EEX is the result of a merger between the power exchanges in Leipzig and Frankfurt in 2002. Now based in Leipzig, the exchange is a platform for trading in power, natural gas, emission rights and coal.

In 2008, the EEX power spot market concluded a joint venture with its French counterpart Powernext to create the EPEX spot market for France, Germany/Austria and Switzerland. The European Electricity Index (ELIX) was launched in October 2010 as the new market index in an integrated European market. However, we prefer to use a more established index that has become the reference in Germany and most of Europe: the Physical Electricity Index (Phelix). Phelix Base is the arithmetic mean of twenty-four spot prices, each characterizing in Euros the price of one MWh today delivered the next day in the market area Germany/Austria. To take account for intraday seasonality, Phelix Peak is the average of the twelve peak load hour spot prices from 8 am until 8 pm for the same market area.

Spot prices are determined through daily auctions by matching supply and demand curves. These curves have very specific shapes due to the intrinsic nature of electricity. The supply curve for electricity is constructed such that each generation unit is stacked, ranked from the lowest (hydropower and nuclear plants) to the highest (less efficient plants and peakers) marginal generation cost. The resulting curve is also called power stack function or merit order of electricity. The

characteristic of this curve is its convexity at the right hand side since it becomes steeper when production moves to more expensive generation units during peak hours for example. The shape of the supply curve is therefore mainly technology-driven (plant efficiency) but economic factors like the price of primary energies (e.g. gas, oil, coal) can also have an impact either on the level of the curve (general price movement) or on the merit order. On the demand side, the level of demand is sensitive to weather and human activity such that it exhibits daily, weekly and yearly seasonality. Despite the recent deregulation and the following increase of competition in electricity markets, the demand curve remains inelastic, as electricity is an essential commodity for human activity.

Because electricity is non-storable, supply and demand have to match at any time. In commodity markets the mean reversion rate of prices is a function of the speed of adjustment of the supply side to 'events' in the market (Pilipovic (2007), p. 24). For this reason, power spot prices tend to exhibit very strong mean reversion and high volatility. Because of the convex shape of the power stack function, spot price jumps tend to occur more frequently to the upside followed by a rapid opposite movement towards the mean level. These jumps are caused by physical events like plant outages creating sudden abrupt changes in the shape of the power stack function, or heat waves on the demand side. As a result, jumps are expected to happen at a certain frequency as a natural behavior of the price series.

Another important specificity of the electricity market is its transmission network as there is no alternative to it for the transportation of electricity. Transmission constraints between interconnected regions exist and may also impact strongly the price dynamics as suggested by Haldrup and Nielsen (2006). Indeed, the price formation is different whether there is congestion or not between interconnected zones operated by different Transmission System Operators (TSO).¹ For example, Germany/Austria is considered as a joint market area except in case of congestion between TSO zones² where spot prices are determined by means of separate auctions for each zone.

Next to the spot market, EEX operates a market for power derivatives in Germany and France. Power derivatives are traded both over-the-counter (OTC) and on exchanges. Though OTC transactions represent the largest volume in the EEX market, we are interested in standardized contracts for their high liquidity and the transparency of their prices. Futures with cash settlement (Phelix futures), futures with physical settlement (Power futures) and options on financial futures (Phelix options) are traded on EEX. Phelix futures are written on Phelix Base or Phelix Peak indices. For Power futures the delivery of power during base or peak load hours at a specified TSO zone constitutes the underlying.

Several reasons lead to an increasing interest in electricity futures. First, futures are used by risk management to hedge against spot price fluctuations during the delivery period. Indeed, futures

¹The TSO is an independent organization responsible for the efficient supply of the total demand of electricity in a particular region. After the deregulation and the following unbundling of vertically integrated power companies in Europe, the TSO remains a regulated entity in order to ensure non-discriminatory access to the grid.

²Amprion GmbH, Transpower Stromübertragungs GmbH, 50hertz Transmission GmbH, EnBW Transportnetze and Austrian Power Grid.

contracts are a way to lock the price in advance for the planned generation/consumption of the year, the quarter, the month and the week with the recent introduction of Phelix week futures so that spot trading is only used to optimize the procurement and sale of power in the short run. Then, futures are also the most natural vehicles to trade power for investors willing to take positions in the market without the physical constraints linked to electricity. For these reasons, the portfolio of electricity 'investors' is mainly consisting of futures.

3 Phelix futures prices: data description and cointegration analysis

3.1 Data description

We consider the price series of three Phelix baseload futures contracts traded on EEX corresponding to monthly, quarterly and yearly maturities with respective delivery periods. The futures are traded for the current and the next nine months (month future), for the next eleven quarters (quarter future) and for the next six years (year future). It seems however relevant to focus on front contracts that account for the majority of futures trading activity at EEX (Wilkins and Wimschulte (2007)). Month contracts are fulfilled by cash settlement where the settlement price is the Phelix Base monthly index, the arithmetic mean of Phelix Base indices for the delivery month. Quarter and year futures contracts are fulfilled by cascading. Cascading means the automatic splitting of long term contracts into contracts with the next shortest maturity/delivery period which together total the volume of the long term contract (Geman (2005), p. 274). For example, three trading days before January 2005 the 2005-year future is divided into three-month futures for January, February and March and three quarter futures for the second, third and fourth quarters. Then, three trading days before April the second quarter contract is divided into April, May and June futures contracts with cash settlement, etc.

The database consists of three daily price series composed of successive nearest contracts over the period 07.01.2002 until 04.14.2010 (yielding 1963 observations).³ The month futures price series is constructed such that the nearest contract month forms the first values for the continuous series until the first business day of the actual contract month. The quarter and year futures series are also composed of nearest contracts but the contract switch over is made on the cascading day. These continuous futures prices and returns (adjusted for contract switches) are depicted in Figure 1.

Table 1 contains descriptive statistics for the percentage returns of Phelix Base monthly index and Phelix Base futures prices where the first four lines give the empirical correlations. We notice the extremely high excess kurtosis of the returns on the index compared to futures returns due to the presence of jumps. As expected, we also observe a decrease in the standard deviations of returns when maturity increases from one day (spot index) to one year (year future). However, a linear relationship between spot and futures returns is not observed; correlations are negative and close to

³Source: Datastream. Series codes: EBMCS00, EBQCS00, EBYCS00.

zero.⁴ The absence of a clear-cut relationship between observed spot and futures returns motivates our choice to consider a model for forecasting futures returns separately from the spot market.

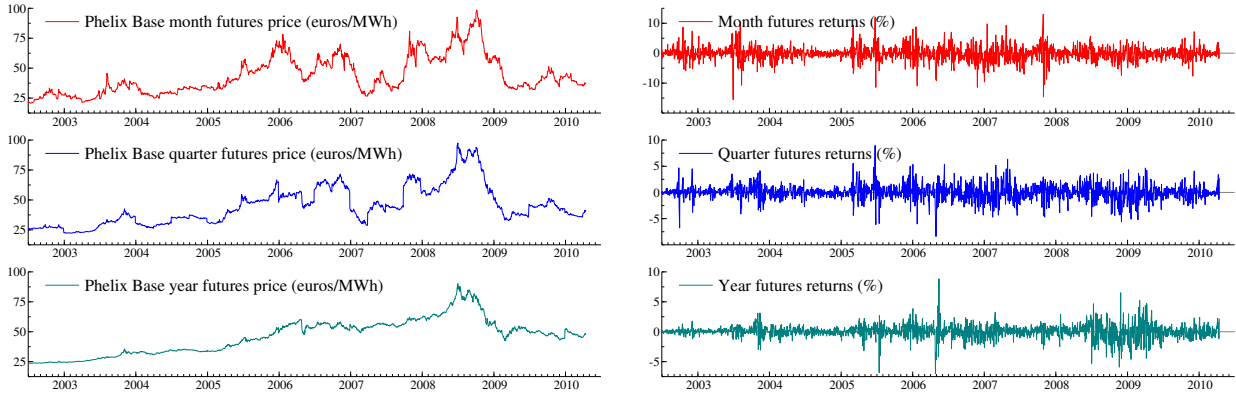


Figure 1: Phelix futures prices and returns (month, quarter, year future)

	Phelix Base	Month Future	Quarter Future	Year Future
Phelix Base	1			
Month Future	-0.005	1		
Quarter Future	-0.032	0.791	1	
Year Future	-0.051	0.559	0.773	1
Mean	-0.014	-0.118	-0.008	0.025
St. Deviation	7.871	2.383	1.462	1.098
Skewness	-1.773	-0.131	-0.149	-0.176
Excess Kurtosis	32.841	4.467	3.541	6.952

Table 1: Descriptive statistics of spot and futures returns (1962 observations). The upper panel shows the sample correlation matrix.

3.2 Cointegration in Phelix futures prices

To simplify estimation, we opt for a two-step approach. In the first step, we model jointly the conditional means of futures log-prices. In the second step (see next Sections) we model the volatility and correlation structure of the residuals of the first step.

Unit root augmented Dickey-Fuller tests applied to the log prices confirm the three series to be integrated of order one and their first differences to be stationary. This result suggests the possible existence of cointegrating relationships between log prices. To filter the series from possible co-movements in the conditional means, we use a vector error correction model (VECM). Based on a

⁴A possible explanation for the negative correlations comes from the very weak persistence of spot price jumps (implied by a strong mean reversion rate). Hence, when a spot jump induces a jump in futures prices (of less amplitude) the price of the futures contract tend to remain at this higher level for a certain period whilst the spot automatically reverts towards a mean level on the next day.

lag-structure analysis of log prices, we specify the following VECM:

$$\Delta y_t = \Pi y_{t-1} + \Gamma \Delta y_{t-1} + u_t, \quad u_t \sim IN(0, \Omega),$$

where $y_t = (y_{Mt} \ y_{Qt} \ y_{Yt})'$ is the vector of log prices for different maturities.⁵ The long-run matrix Π can be factorized into $\alpha\beta'$ where α (of dimension $3 \times r$) contains the speed of adjustment to disequilibrium coefficients and β (of dimension $3 \times r$) contains the coefficients of the r cointegration relationships such that $\beta'y_t$ is stationary. The trace rank test of Johansen (1991) indicates the presence of two cointegration vectors. The matrices α and β are identified by imposing $\beta = (I_2 \ B)'$. Their maximum likelihood estimates are:

$$\hat{\beta} = \begin{pmatrix} 1 & 0 \\ 0 & 1 \\ -0.898 & -0.960 \end{pmatrix} \quad \hat{\alpha} = \begin{pmatrix} -0.010 & 0.016 \\ -0.004 & 0.009 \\ 0.000 & 0.001 \end{pmatrix}.$$

Given the p-value of 64% for the likelihood ratio test, we conclude that the last row of the alpha matrix ($\alpha_{31} \ \alpha_{32}$) is not rejected to be null. Year futures returns are therefore not subject to error-correction, and can be interpreted as the common trend of the system. Integrating this restriction, we get $\hat{\beta}_1 = (1 \ 0 \ -0.91)$ and $\hat{\beta}_2 = (0 \ 1 \ -0.968)$ as estimated cointegration vectors.

As parsimonious VECM model (after removing non significant variables at the 5% level) we get

$$\begin{aligned} \Delta y_{Mt} &= 0.066 + 0.121 \Delta y_{Mt-1} - 0.010 \hat{\beta}'_1 y_{t-1} + 0.014 \hat{\beta}'_2 y_{t-1} + \epsilon_{Mt} \\ &\quad (0.092) \quad (0.033) \quad (0.004) \quad (0.005) \\ \Delta y_{Qt} &= 0.028 + 0.15 \Delta y_{Qt-1} - 0.003 \hat{\beta}'_1 y_{t-1} + 0.006 \hat{\beta}'_2 y_{t-1} + \epsilon_{Qt} \\ &\quad (0.052) \quad (0.028) \quad (0.002) \quad (0.002) \\ \Delta y_{Yt} &= 0.026 + 0.071 \Delta y_{Qt-1} + \epsilon_{Yt}, \\ &\quad (0.025) \quad (0.021) \end{aligned}$$

where White's heteroskedastic consistent standard errors are reported in parentheses. Note that we keep the non-significant constants in the equations to obtain zero-mean residuals for the next step devoted to multivariate volatility modeling.

Multivariate GARCH modeling of the covariance matrix of the above VECM residuals is principally motivated by two observations. First, the autocorrelation functions of squared residuals show evidence of dependence that could be typically captured in a GARCH model. Second, the high positive correlations between the residuals - 0.56 for month-year futures, 0.77 for quarter-year, and 0.79 for month-quarter - give a clear incentive to consider a joint model for the volatility of the series.

⁵Note that y_{t-1} , like the returns, is adjusted for contract switches.

4 Standard DCC models

Multivariate GARCH models are increasingly used thanks to recent progresses in their specification, the associated inference tools, and their increased availability in econometric software; see Bauwens et al. (2006), Silvennoinen and Teräsvirta (2009) for surveys of these models. For electricity futures as much as for other financial returns, understanding the co-movements in their second-order moments is of great practical importance for portfolio and risk management purposes. Portfolio allocation, risk measures and hedging strategies can be significantly improved by taking into account the co-volatilities between futures of different maturities.

In the following, we consider the vector ϵ_t of "demeaned" return series of electricity futures which are the VECM residuals of the previous section. In general, a multivariate GARCH model for T observations on a vector ϵ_t of n elements is defined by

$$\epsilon_t = H_t^{1/2} z_t, \quad z_t \sim iid(0, I_n), \quad t = 1, 2, \dots, T, \quad (1)$$

where $H_t^{1/2}$ is any $n \times n$ full rank matrix such that $\text{Var}(\epsilon_t | \mathcal{F}_{t-1}) = H_t^{1/2} (H_t^{1/2})' = H_t$. The model definition is completed by specifying the information set \mathcal{F}_{t-1} and the way in which the conditional covariance matrix H_t depends on \mathcal{F}_{t-1} through a finite number of parameters. By default \mathcal{F}_{t-1} is the sigma field generated by $\{\epsilon_{t-1}, \epsilon_{t-2}, \dots\}$ but it may be augmented by additional variables as we do in Section 6.2.

Different specifications for H_t were tested and a ranking according to Bayesian and Akaike information criteria revealed the Dynamic Conditional Correlation (DCC) model of Engle (2002) and the corrected Dynamic Conditional Correlation (cDCC) model of Aielli (2009) to outperform other models for the ϵ_t series of residuals obtained in the previous section. For this reason, the results we present in this paper are based on this class of models though we do not reject the possibility that other models may perform better, for example when the number of series increases.

In conditional correlation models the conditional covariance matrix H_t is expressed as $H_t = D_t R_t D_t$ where $D_t = \text{diag}(h_{11t}^{1/2}, \dots, h_{nnt}^{1/2})$ is a matrix collecting the univariate conditional volatilities on its diagonal and R_t is a correlation matrix. If the distribution of z_t in (1) is assumed Gaussian, the DCC model allows for a two-stage estimation procedure, where in the first stage the parameters of the univariate conditional variance processes are estimated, and in the second stage the parameters of the conditional correlation process are estimated conditionally on the parameter estimates obtained in the first stage.

In the first stage, we notice that information criteria decrease when replacing the standard GARCH specification by the asymmetric GARCH model (GJR) of Glosten et al. (1993). The conditional variance h_{iit} following a GJR process is defined as

$$h_{iit} = \omega_i + \alpha_i \epsilon_{it-1}^2 + \beta_i h_{iit-1} + \gamma_i \epsilon_{it-1}^2 I_{\{\epsilon_{it-1} < 0\}} \quad (2)$$

where $I_{\{\epsilon_{it} < 0\}}$ is a dummy variable equal to one when the past shock is negative, $\alpha_i, \beta_i \geq 0$, and $\alpha_i + \beta_i + 0.5\gamma_i < 1$. The parameter γ_i is expected to be positive in equity markets and is usually interpreted as the leverage effect parameter where the conditional volatility is affected more strongly by negative shocks ($\epsilon_{it} < 0$) than positive shocks of the same size. The negative sign of the estimated GJR parameter for month and quarter futures in Table 2 (left part) suggests the presence of an “inverse leverage effect” where positive shocks to returns amplify the conditional variance more than negative shocks. The absolute value of the estimate of γ is decreasing with the maturity and γ is not significant for the year future. Knittel and Roberts (2005) also find this effect on power spot prices from California. They attribute the inverse leverage effect in electricity returns to the convexity of the power stack function where positive demand shocks have a larger impact on price volatility than negative demand shocks.

	GJR (eq (2))		GJR (eq (4))	
Month Baseload Future	Coefficient	Std. error	Coefficient	Std. error
Cst (ω)	0.068	0.028	-	-
ARCH (α)	0.232	0.037	0.296	0.032
GARCH (β)	0.836	0.024	0.724	0.034
GJR (γ)	-0.126	0.032	-0.164	0.033
Log-likelihood:	-3862.30		-2293.23	
	GJR (eq (2))		GJR (eq (4))	
Quarter Baseload Future	Coefficient	Std. error	Coefficient	Std. error
Cst (ω)	0.020	0.008	-	-
ARCH (α)	0.215	0.030	0.211	0.027
GARCH (β)	0.838	0.020	0.755	0.029
GJR (γ)	-0.087	0.029	-0.093	0.032
Log-likelihood:	-3019.41		-2420.46	
	GJR (eq (2))		GJR (eq (4))	
Year Baseload Future	Coefficient	Std. error	Coefficient	Std. error
Cst (ω)	0.006	0.004	-	-
ARCH (α)	0.159	0.024	0.136	0.013
GARCH (β)	0.856	0.023	0.823	0.018
Log-likelihood:	-2393.37		-2303.15	

Table 2: Conditional variance parameter estimates for ϵ_t (eq (2), left part) and ξ_t (eq (4), right part). Sample period: 01.09.2003-04.14.2010 (1831 observations)

Despite the negative GJR parameters, the estimates imply non-existence of the unconditional variances ($\alpha + \beta + \gamma/2 > 1$). We suspect the persistence to be overestimated due to a changing unconditional variance over time. Extensions of the univariate GARCH model to deal with spurious persistence have been proposed, such as component (Engle and Lee (1999); Bauwens and Storti (2009)), regime switching (Haas et al. (2004b); Bauwens et al. (2010)), mixture (Haas et al. (2004a)) and spline (Engle and Rangel (2008)) GARCH models.

The second stage is devoted to the estimation of conditional correlation parameters. The DCC structure is defined by

$$Q_t = (1 - a - b)\bar{Q} + au_{t-1}u'_{t-1} + bQ_{t-1} \quad (3)$$

where $a+b < 1$, $a, b \geq 0$, $u_{it} = \epsilon_{it}/\sqrt{h_{iit}}$ are the "degarched" errors, Q_t is a $n \times n$ symmetric positive definite matrix, \bar{Q} is a parameter matrix and it is assumed that $\bar{Q} = E(u_t u'_t)$. Then correlations are obtained by transforming this to

$$R_t = (\text{diag}Q_t)^{-1/2}Q_t(\text{diag}Q_t)^{-1/2}.$$

However, Aielli (2009) proved the estimation of \bar{Q} by the empirical covariance of u_t to be inconsistent since

$$E(u_t u'_t) = E(E(u_t u'_t | \mathcal{F}_{t-1})) = E(R_t) \neq E(Q_t).$$

Aielli proposes a corrected specification of Q_t :

$$Q_t = (1 - a - b)\bar{Q} + a\tilde{u}_{t-1}\tilde{u}'_{t-1} + bQ_{t-1}$$

where $\tilde{u}_t = P_t u_t$ and $P_t = \text{diag}(q_{11t}^{1/2}, \dots, q_{nnt}^{1/2}) = (\text{diag}Q_t)^{1/2}$, so that, by construction, \bar{Q} is the unconditional covariance of \tilde{u}_t .

The DCC and cDCC models are however empirically very similar.⁶ Table 3 collects the second stage estimation results for the parameters of the DCC model. Only a slight increase of the likelihood function to 1952.83 is observed for the cDCC model and the measure for the persistence of shocks in correlations is high ($a + b$ is close to one) in both models.

DCC	Coefficient	Std. error
\bar{Q}_{MQ}	0.795	0.020
\bar{Q}_{MY}	0.621	0.034
\bar{Q}_{QY}	0.808	0.021
a	0.044	0.013
b	0.915	0.030
Log-likelihood:	1949.18	

Table 3: Standard DCC parameter estimates (eq (3)). Sample period: 01.09.2003-04.14.2010 (1831 observations)

Some empirical results tend to underline the need for a more flexible modeling of the conditional correlations too. For example, bivariate estimations lead to very different parameters for the dynamics of each pair of correlations. Besides, estimations on time subsamples give different constant correlation levels. We are therefore interested in introducing flexibility in these two directions;

⁶As for the conditional variances, the standard (c)DCC process for conditional correlations may be improved allowing for asymmetries (Cappiello et al. (2006)). The presence of asymmetries in Phelix futures correlations is however not significant at the 5% level.

allowing for asset-specific correlation dynamics and time-varying unconditional correlation levels. Developments of this kind are recent and show the growing interest of flexible modeling of conditional correlations. On one hand, asset-specific parameters for dynamic conditional correlations have already been introduced with the quadratic flexible DCC model of Billio and Caporin (2009) and the generalized DCC model of Hafner and Franses (2009). On the other hand, several models deal with changing levels in constant correlations like the regime switching dynamic correlation model of Pelletier (2006), the component DCC model of Colacito et al. (2009), the smooth transition conditional correlation model of Silvennoinen and Teräsvirta (2005), the factor-spline-GARCH DCC model of Rangel and Engle (2009), and the multivariate multiplicative volatility model of Hafner and Linton (2010).

Evidence from first and second stage estimation, such as the extreme persistence, suggests a model that allows for smooth changes in the unconditional volatilities and correlations of electricity futures. These changes are induced by different factors affecting the market environment or the market structure like changing energy prices, growing market size, new technologies or the arrival of new market participants, new products, etc. In the model of Hafner and Linton (2010) the covariance matrix H_t is decomposed into conditional and unconditional components where the unconditional component is a deterministic function of time estimated by a kernel method and the conditional component is a BEKK model. However, we prefer to keep the DCC structure for the conditional covariance matrix since it was shown to perform significantly better in terms of fit. In the next section, we present a new multiplicative model that extends the multivariate multiplicative volatility model of Hafner and Linton (2010) to the DCC framework.

5 Multiplicative DCC model

Before applying it to electricity futures, we define the multiplicative DCC (mDCC) model in its most general form. The idea is to decompose the conditional covariance matrix of ϵ_t into an unconditional component that can change smoothly through time, and a conditional component that captures the short-run dynamic structure typical of multivariate GARCH processes.

To achieve this, the square root matrix $H_t^{1/2}$ in (1) is itself written as the product of two square root matrices $\Sigma(t/T)^{1/2}$ and $G_t^{1/2}$ such that

$$H_t = \Sigma(t/T)^{1/2} G_t^{1/2} (G_t^{1/2})' [\Sigma(t/T)^{1/2}]' = \Sigma(t/T)^{1/2} G_t [\Sigma(t/T)^{1/2}]'$$

is positive-definite, symmetric, and of full rank. The matrix G_t is specified as a DCC process to capture the short run GARCH dynamics. By assuming, for identification, that $E(G_t) = I_n$, it follows that

$$\text{Var}(\epsilon_t) = E(H_t) = \Sigma(t/T)^{1/2} [\Sigma(t/T)^{1/2}]' = \Sigma(t/T)$$

so that $\Sigma(t/T)$ is the unconditional "long run" covariance matrix that is assumed to be a determin-

istic and smooth function of time.

The idea behind this formulation is to combine the estimation by kernel of the long run covariance matrix with maximum likelihood estimation of the short run parameters in G_t . By further splitting the latter into the two usual estimation stages of the DCC model, the estimation procedure comprises three stages where an initial stage is added for the estimation of the unconditional covariance.

In the first stage, the unconditional covariance matrix is estimated by the Nadaraya-Watson estimator

$$\hat{\Sigma}(\tau) = \frac{\sum_{t=1}^T K_h\left(\frac{t}{T} - \tau\right) \epsilon_t \epsilon_t'}{\sum_{t=1}^T K_h\left(\frac{t}{T} - \tau\right)}$$

where $\tau \in [0, 1]$, $K_h(\cdot) = (1/h)K(\cdot/h)$, $K(\cdot)$ is a kernel function, and h is a positive bandwidth parameter. Unconditional correlations are then estimated by

$$\hat{\rho}_{ij}(\tau) = \frac{\hat{\Sigma}_{ij}(\tau)}{\sqrt{\hat{\Sigma}_{ii}(\tau)\hat{\Sigma}_{jj}(\tau)}}.$$

The standardized returns derived from the first stage estimation, defined by

$$\xi_t = \hat{\Sigma}(\tau)^{-1/2} \epsilon_t,$$

have asymptotically as unconditional covariance an identity matrix, and as conditional covariance the matrix G_t , i.e. $E(\xi_t \xi_t') = I_n$ and $E(\xi_t \xi_t' | \mathcal{F}_{t-1}) = G_t$.

In the second stage, the conditional variance parameters for the elements of ξ_t are estimated by maximum likelihood. Like for the standard DCC model, any univariate GARCH process satisfying appropriate stationarity conditions and non-negativity constraints can be used. We shall use for our application in Section 6 the GJR model as in (2) with ξ_{it} replacing ϵ_{it} and imposing a unit variance:

$$g_{iit} = (1 - \alpha_i - \beta_i - 0.5\gamma_i) + \alpha_i \xi_{it-1}^2 + \beta_i g_{iit-1} + \gamma_i \xi_{it-1}^2 I_{\{\xi_{it-1} < 0\}}, \quad (4)$$

where $g_{iit} = \text{Var}(\xi_{it} | \mathcal{F}_{t-1})$. The Gaussian log-likelihood for stage two is

$$l_2 = -\frac{1}{2} \sum_{i=1}^n \sum_{t=1}^T \left[\log(g_{iit}) + \frac{\xi_{it}^2}{g_{iit}} \right].$$

The second-stage "degarched" residuals, defined by

$$u_t = D_t^{-1} \xi_t,$$

where $D_t = \text{diag}\left(g_{11t}^{1/2}, \dots, g_{nnt}^{1/2}\right)$, have consequently an identity matrix as unconditional covariance matrix and unit conditional variances but are conditionally correlated, i.e. $E(u_t u_t') = I_n$ and $E(u_t u_t' | \mathcal{F}_{t-1}) = R_t$, where R_t is the conditional correlation matrix.

In the third stage, the parameters of the conditional correlation matrix are estimated. The proposed dynamic correlation structure is a DCC model for the second-stage residuals

$$Q_t = (1 - a - b)I_n + au_{t-1}u'_{t-1} + bQ_{t-1}, \quad (5)$$

where $a + b < 1$ and $a, b \geq 0$, and the conditional correlations are obtained from

$$R_t = (\text{diag}Q_t)^{-1/2}Q_t(\text{diag}Q_t)^{-1/2}.$$

This DCC model *à la Engle* is not subject to Aielli's critique, since

$$E(Q_t) = (1 - a - b)I_n + aE(u_{t-1}u'_{t-1}) + bE(Q_{t-1}) = I_n$$

as $E(u_{t-1}u'_{t-1}) = E(u_tu'_t) = I_n$ by construction. However a cDCC version, with $\tilde{u}_{t-1} = P_t u_{t-1}$ replacing u_{t-1} in equation (5), where $P_t = (\text{diag}Q_t)^{1/2}$, can also be used and has the same property.⁷ The Gaussian log-likelihood for stage three is

$$l_3 = -\frac{1}{2} \sum_{t=1}^T [\log(|R_t|) + u'_t R_t^{-1} u_t - u_t u'_t].$$

Finally, if the model is correctly specified, both unconditional and conditional covariance matrices of the third-stage residuals $\hat{z}_t = \hat{H}_t^{-1/2} \epsilon_t$ are asymptotically equal to the identity matrix, which can be used for misspecification diagnostics.

6 Application to Phelix futures

6.1 Smoothly time-varying unconditional covariance matrix

The proposed mDCC model allows for a long-term component that is slowly changing over time. The bandwidth parameter h serves to identify long term and short-term movements. The smaller the bandwidth, the larger the size of movements that is captured by the long-term component and the smaller the amplitude of short-term conditional movements.

Several procedures are available to select the bandwidth based on the minimization of quadratic error measures for a regression curve. For nonparametric regression, a common criterion for choosing the optimal bandwidth is the least squares cross-validation criterion. Härdle (1990) shows that the procedure amounts to choosing the bandwidth that minimizes the sum of squared differences between model predictions and observed data, where small values for the bandwidth are penalized.⁸ Since the long-term covariance matrix is not observed, we take a six-month rolling covariance as the reference for the computation of squared differences. The optimal bandwidth is the bandwidth

⁷Indeed, $E(Q_t) = (1 - a - b)I_n + aE(\tilde{u}_{t-1}\tilde{u}'_{t-1}) + bE(Q_{t-1})$ with $E(\tilde{u}_{t-1}\tilde{u}'_{t-1}) = E[E(P_{t-1}u_{t-1}u'_{t-1}P'_{t-1}|\mathcal{F}_{t-2})] = E[P_{t-1}R_{t-1}P'_{t-1}] = E(Q_{t-1})$ and $E(Q_{t-1}) = E(Q_t)$ imply that $E(Q_t) = I_n$.

⁸As penalty function we use Rice's T , defined as $\Xi_T(u) = (1 - 2u)^{-1}$.

that minimizes this criterion and is equal to 0.05 for a Gaussian kernel.

To assess the quality of fit of long-term variances and correlations, estimated unconditional levels are compared with alternative measures of long-term variances and correlations. In Figures 2 and 3, we compare estimated unconditional variances and correlations (black smooth lines) with their six-month realized levels (black dots) and their six-month rolling levels (black discontinuous lines). The light grey lines are the total levels of variances and correlations including unconditional and conditional components. In Figure 4, we present pointwise confidence bands (black dashed lines) at 95% confidence level for the kernel estimator of the covariance as defined in Härdle (1990, p. 127). The level of confidence intervals gives a clear indication to reject the hypothesis of constant unconditional variance and covariance levels.

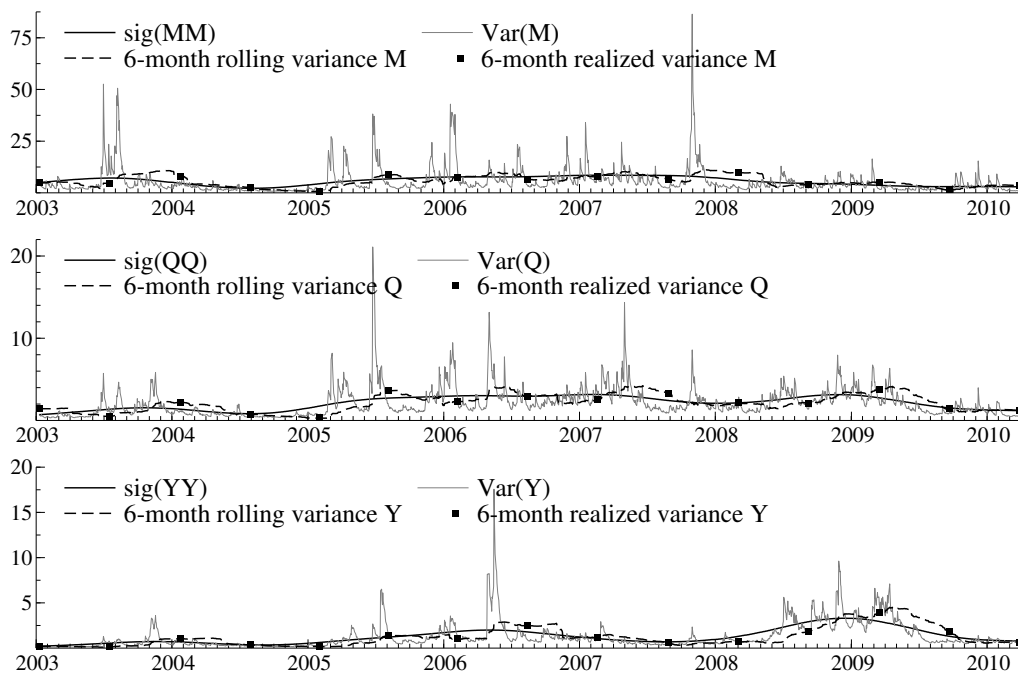


Figure 2: Unconditional variances (month, quarter, year future). The nonparametric unconditional variance of futures contracts of maturity i is $sig(ii) = \hat{\Sigma}_{ii,t}$. The estimated total variance of contract i is $Var(i) = \hat{H}_{ii,t}$.

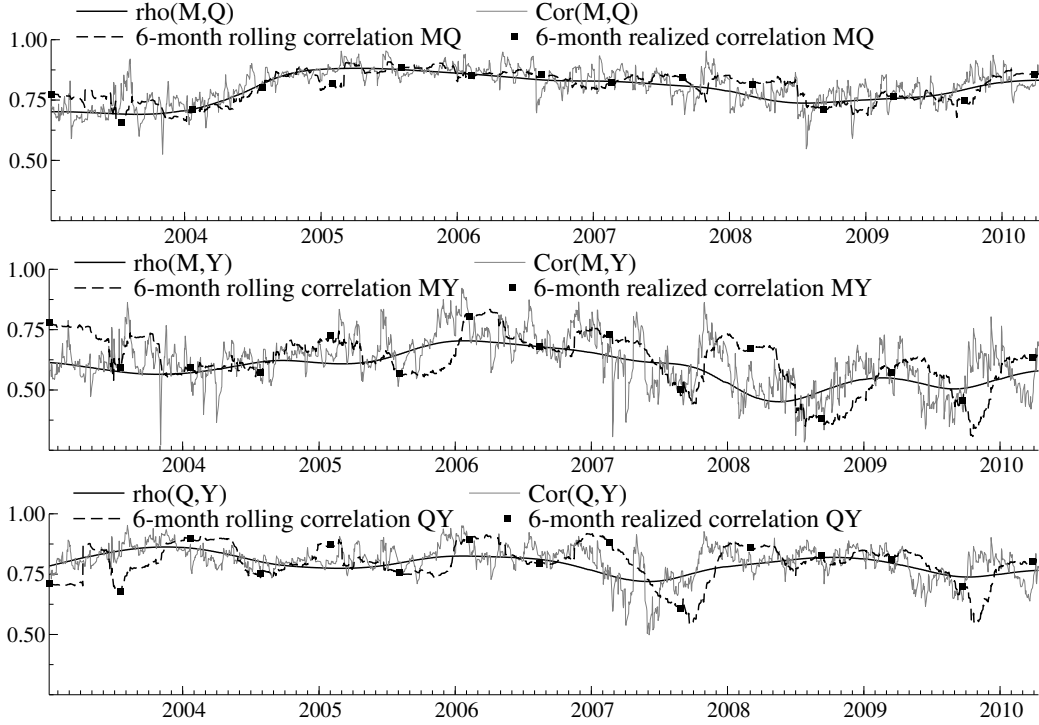


Figure 3: Unconditional correlations (month-quarter, month-year, quarter-year). The nonparametric unconditional correlation between contracts of maturity i and contracts of maturity j is $\rho(i, j) = \hat{\rho}_{i,j,t}$ for $i \neq j$. The estimated total correlation between contracts i and j is $Cor(i, j) = \hat{H}_{i,j,t} / (\hat{H}_{i,i,t} \hat{H}_{j,j,t})^{1/2}$ for $i \neq j$.

Changing regimes in variances and covariances should coincide with structural changes in power markets. Figure 5 shows the annual growth of the total volume of electricity consumed in Germany from 2004 to 2009.⁹ The period of high demand growth of 2006-2008 has led to increasing trading volumes of derivatives on the EEX market. While the decline of consumption after 2008 may be attributable to the downturn of the industrial sector after the 2008 financial crisis, the period of consumption growth between 2005-2008 is mainly driven by residential and tertiary sectors. According to a report published by the Joint Research Center of the European Commission,¹⁰ the increase of residential consumption in the European Union is due to many factors among which the widespread use of traditional appliances (refrigerators, dishwashers, personal computers, etc.) and the introduction of new consumer electronics and information and communication technology equipment. As already mentioned, positive demand growth has an impact on the volatility of electricity prices. Like for other commodities, higher volatility may be caused by a probable shortage of the resource. For electricity, a shortage is implied by generation and transmission constraints. As a result, month and quarter futures display a mode in their variances and covariances in 2007; a year

⁹Source: Datamonitor, Electricity in Germany: industry profile, October 2008 and August 2010 (ref. 0165-0663).

¹⁰Source: JRC, Electricity Consumption and Efficiency Trends in the Enlarged European Union - Status Report 2006 - (ref. JRC36429).

of maximal demand growth in Germany. More generally, the period 2006-2008 witnesses both high power consumption growth in Germany and high variances/covariances for all futures products.

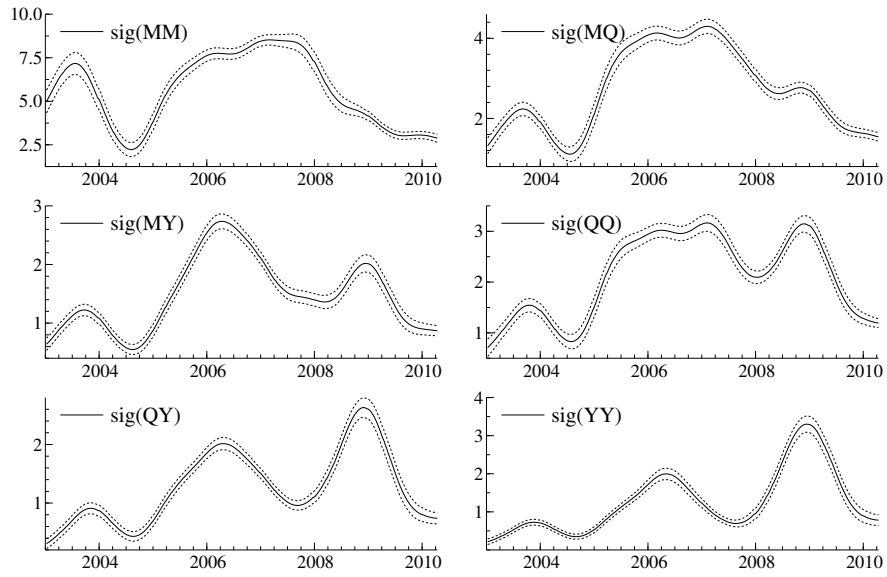


Figure 4: Unconditional covariance ($h = 0.05$) and confidence intervals. The unconditional covariance of contracts i and j is $sig(ij) = \hat{\Sigma}_{ij,t}$ for all i, j .

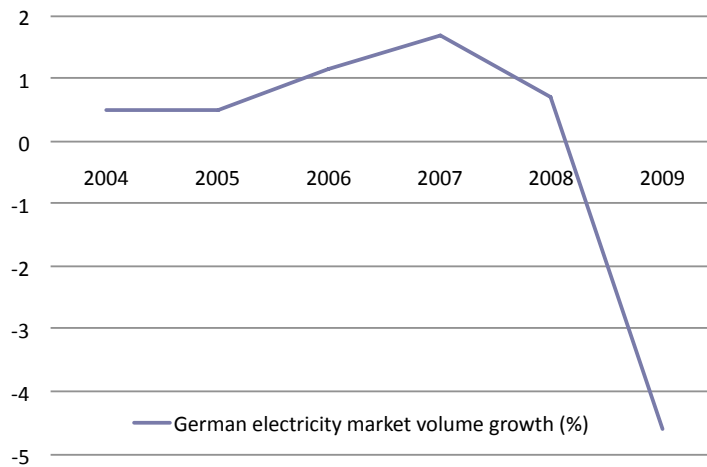


Figure 5: German electricity consumption volume growth

In 2009, we observe a volatility bump in quarter and year futures, and in their co-volatility, see Figure 6. On the same figure, we observe a similar pattern in the volatilities of the S&P 500

index and of the Brent spot price¹¹ following the 2008 financial crisis. Nonparametric estimates of variances of S&P 500 and Brent spot returns¹² are taken as proxies for the volatility of financial and oil markets, respectively. The volatility of S&P 500 reached extreme levels after the announcement of Lehman Brothers bankruptcy in September 2008. The following economic recession caused oil prices to plummet after a long-term trend of slowly increasing prices. This sudden drop induced a maximal volatility of Brent returns in late 2008/early 2009 corresponding to the volatility bump we observe for quarter and year Phelix futures. As a result, the 2009 bump observed for the volatility of quarter and year electricity futures is related to the high volatility of oil prices during the 2008/2009 recession period.

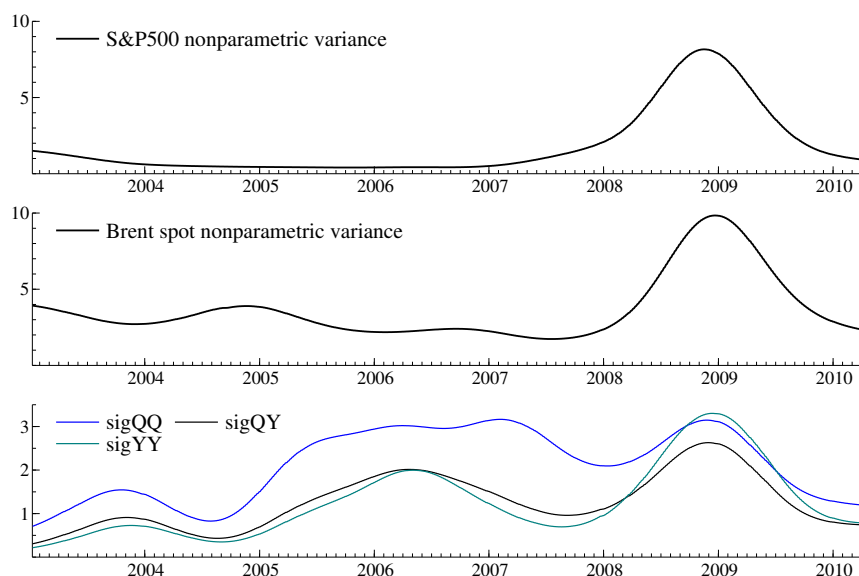


Figure 6: S&P500 and Brent spot variance estimates compared to estimates of unconditional variances of quarter and year futures and their covariance.

The consumption growth and the economic recession are certainly not the unique elements to explain the long-term level of the variances and covariances of electricity futures. Other long-term factors may be responsible for these changes, like political decisions in favor of 'cleaner' electricity, the level of primary energy prices, the launch of new generation technologies or the introduction of emission rights changing the merit order, a raising awareness of resource scarcity affecting the risk aversion of investors, new regulations ensuring the independence of TSOs, etc. The arrival of new market participants, new financial products, mergers, acquisitions and other alliances also change the market structure by rebalancing the actual forces governing the market. The integration of European power exchanges like the merger of German and French spot exchanges in 2008 may also

¹¹Source: U.S. Energy Information Administration (EIA).

¹²Estimated with a Gaussian kernel, with $h=0.05$

have impacted the variance-covariance levels of futures. Risk aversion, market power or the impact of some market trends are however hard to measure quantitatively. For this reason, the mDCC model is convenient as it is exclusively based on data evidence and does not require identifying and measuring the variables influencing the long-term level of the variances and covariances.

6.2 A seasonal congestion model for conditional variances

We turn to the modeling and the estimation of conditional variances of electricity futures. The right part of Table 2 gathers the results of the (second stage) estimation of the conditional GJR variances given by (4). Compared to the estimates of the standard GJR variances on the left hand, we notice the substantial reduction of the persistence of each univariate process and the increased absolute value of the “inverse leverage” parameters for month and quarter futures. As for the standard model, the leverage parameter is not significant for the year future and is therefore not included.

With the decomposition of the variances into long and short term components we are able to identify variables exclusively explaining short-term movements in the volatility of electricity futures. Next to supply and demand shocks, grid transmission shocks may influence the volatility of electricity futures. As already mentioned, the spot price formation at EEX is different whether there is congestion between TSO zones (inside the same market area) or not. Haldrup and Nielsen (2006) model Nord Pool spot prices with directional congestion as the state variable in a regime-switching model. Their proxy for congestion is the difference of spot prices between Nord Pool regions where the region with the highest price is the region with excess demand. Besides, transmission constraints also exist between countries or market areas and may also impact the short-term volatility of electricity futures. We adapt the congestion variable of Haldrup and Nielsen to account for the impact of international congestion on the conditional variances. The proxy employed for congestion is the squared difference of log baseload or peakload indices between EEX and neighboring markets such as APX for the Netherlands, Nord Pool West and East Denmark, GME for Italy, Powernext for France and the Dow Jones index for Swiss electricity prices.¹³ These variables are incorporated additively in the GJR process (4):

$$g_{iit} = \phi_i + \alpha_i \xi_{it-1}^2 + \beta_i g_{iit-1} + \gamma_i \xi_{it-1}^2 I_{\{\xi_{it-1} < 0\}} + \sum_{k=1}^K \delta_{ik} [\log(p_{EEX,t-1}) - \log(p_{k,t-1})]^2 + \kappa_i (T_{MD} - t) \quad (6)$$

where

$$\phi_i = 1 - \alpha_i - \beta_i - 0.5\gamma_i - \sum_{k=1}^K \delta_{ik} T^{-1} \sum_{t=2}^T [\log(p_{EEX,t-1}/p_{k,t-1})]^2 - \kappa_i T^{-1} \sum_{t=1}^T (T_{MD} - t),$$

$p_{k,t-1}$ is the index of market k at time $t - 1$, K is the number of adjacent market areas and $(T_{MD} - t)$ is the number of days before the first day of the next delivery period of the month future.

¹³The list is not exhaustive. These price indices are available in Datastream.

The parameter κ_i captures the seasonality attached to the expiry date of the futures contract. A negative κ_i is a manifestation of the so-called ‘‘Samuelson effect’’: futures volatility increases when they approach their maturity date (Samuelson (1965)). Only the seasonality of the month contract is found to be significant to explain the volatility of Phelix futures returns. We know that the month future is directly followed by a delivery period while other futures are cascading at maturity. Since the month Phelix contract is still traded during the delivery month we prefer to call this effect a day-to-delivery effect rather than a Samuelson (day-to-maturity) effect.

The congestion variables are lagged by one day to allow for forecasting and their selection is based on BIC minimization for the second stage estimation. Estimation results of the selected congestion models accounting for delivery seasonality are presented in Table 4 (left part).¹⁴ The parameter estimates obtained with the seasonal congestion model can be compared with the estimates obtained with a GJR model without exogenous variables for the same sample period (right part of Table 4).

	seasonal congestion GJR		GJR	
Month Baseload Future	Coefficient	Std. error	Coefficient	Std. error
ARCH (α)	0.250	0.029	0.285	0.037
GARCH (β)	0.747	0.032	0.709	0.041
GJR (γ)	-0.116	0.035	-0.117	0.039
Congestion (δ_{Swiss})	0.193	0.087	-	-
Day-to-delivery (κ)	-0.007	0.001	-	-
Log-likelihood:	-1826.85		-1850.53	
	seasonal congestion GJR		GJR	
Quarter Baseload Future	Coefficient	Std. error	Coefficient	Std. error
ARCH (α)	0.200	0.028	0.203	0.029
GARCH (β)	0.762	0.030	0.759	0.033
GJR (γ)	-0.090	0.034	-0.076	0.036
Congestion ($\delta_{FR Peak}$)	0.431	0.206	-	-
Day-to-delivery (κ)	-0.008	0.002	-	-
Log-likelihood:	-1918.45		-1936.80	
	seasonal congestion GJR		GJR	
Year Baseload Future	Coefficient	Std. error	Coefficient	Std. error
ARCH (α)	0.144	0.015	0.134	0.013
GARCH (β)	0.811	0.021	0.827	0.019
Congestion ($\delta_{E.DK Peak}$)	0.061	0.025	-	-
Log-likelihood:	-1837.56		-1841.83	

Table 4: Conditional variance parameter estimates for ξ_t , eq (6) and eq (4). Sample period: 06.23.2004-04.14.2010 (1467 observations)

¹⁴The likelihood values of Table 4 are not comparable with those of Table 2 because of the reduction of the estimation sample to 1467 observations. This is due to the lack of availability of the Powernext baseload index series before 06.23.2004.

From the results of the seasonal congestion model, we first notice that the congestion and day-to-delivery parameters are all significant at the 5% level. Congestion parameter estimates are all positive and day-to-delivery ones are negative as expected. The seasonality associated with the delivery of the month contract is strongly significant for month and quarter futures and is excluded from the yearly futures equation as it is not significant at 5%. The log-likelihood value increases significantly when we incorporate congestion and seasonality variables. It comes out that different markets influence Phelix futures according to their maturity; the month future reacts to congestion with Switzerland (*Swiss*) whilst quarter and year futures are subject to transmission shocks during the day from France (*FR Peak*) and East Denmark (*E.DK Peak*) respectively.

Simulations of conditional variances using the parameter estimates of the seasonal congestion GJR are also better able to replicate empirical (estimated) variances compared to the simulations based on the GJR model. When simulating the variances using the GJR model without exogenous variables, the mean squared error with respect to the estimated variances from the same model is equal to 3.67. Adding seasonal and congestion variables to simulate the variances, the mean squared error with respect to the estimated variances using the seasonal congestion GJR model drops to 3.31.¹⁵ The reason for this improvement mostly lies in the presence of exogenous congestion variables that force the simulation of jumps to occur at the same time as the estimated jumps.

6.3 Asset-specific dynamic conditional correlations

The third and last stage of the estimation procedure consists in the estimation of the process of conditional correlations between pairs of electricity futures contracts. The DCC estimated parameters are reported in Table 5.¹⁶ We have shown in Section 5 that both DCC and cDCC models are consistent in the multiplicative framework. They also give very similar estimates but the log-likelihood of the cDCC model (35.82) is slightly lower than the DCC log-likelihood (38.76) in this case. The estimate of $a + b$ of the mDCC model (about 0.88) is lower than in the standard DCC model (about 0.95)¹⁷ that does not have a changing unconditional level of the covariance matrix, implying a much smaller persistence of conditional correlations.

We have already mentioned that bivariate estimations for the standard DCC model lead to very different estimates of the parameters for the dynamics of the different pairs of correlations. Though the model was originally conceived for a large number of assets, the generalized DCC (GDCC) of Hafner and Franses (2009) appears also useful in the present context. The conditional correlation structure of the mGDCC model is

$$Q_t = (u' - aa' - bb') \odot I_n + aa' \odot u_{t-1}u'_{t-1} + bb' \odot Q_{t-1}$$

¹⁵Simulation study based on unique simulation paths with the same starting values and the same generated random numbers.

¹⁶Note that the estimates of conditional correlation parameters reported in the next tables are all conditional on second stage estimation using the GJR model capturing congestion and seasonality effects (eq 6).

¹⁷Different from the estimate of 0.96 in Table 3 because of the different sample period used.

where ι is a vector of 1s, a and b are vectors of N parameters each, such that $a_i^2 + b_i^2 < 1$ and $a_i, b_i \geq 0$. Hence $(\iota' - aa' - bb') \odot I_n$ is positive semidefinite¹⁸ for all a and b ensuring a positive definite Q_t . Based on a likelihood-ratio test, we consider a simplified version of the GDCC model, where only the elements of a differ:

$$Q_t = (\iota' - aa' - bI_n) \odot I_n + aa' \odot u_{t-1}u'_{t-1} + b^2Q_{t-1}, \quad (7)$$

where b is now a scalar. The mGDCC parameter estimates are provided in Table 6. The estimate of the first element of a is much smaller than for the last two elements.

We show the mDCC and mGDCC short-term conditional correlations of second stage residuals u_t in Figure 7. Notice that they fluctuate around zero since the long run changing level has been removed by the estimation of the long run component. While the mDCC correlations have by assumption the same dynamics, we see that the correlations of the mGDCC model exhibit different patterns. For the correlation process between month and quarter futures, there seems to be no considerable change between mDCC and mGDCC correlation processes. Compared to the mDCC parameter a , the lower parameter related to the month future (a_M^2) in the mGDCC process forces correlations to concentrate more around the mean but this effect is counterbalanced by a higher parameter for the quarter future (a_Q^2) that amplifies correlation movements. The same observation is applicable for the conditional correlations between month and year futures. The largest change is observed in quarter-year correlations with a higher persistence and amplified movement for short run correlation dynamics. In this case, there is no balancing effect since both parameters (a_Q^2 and a_Y^2) have increased compared to the a parameter of the mDCC process.

mDCC	Coefficient	Std. error
a	0.067	0.010
b	0.812	0.031
Log-likelihood:	38.76	

Table 5: mDCC parameter estimates (eq (5)). Sample period: 06.23.2004-04.14.2010 (1467 observations)

mGDCC	Coefficient	Std. error
a_M^2	0.035	0.013
a_Q^2	0.116	0.036
a_Y^2	0.070	0.027
b^2	0.804	0.031
Log-likelihood:	41.55	

Table 6: mGDCC parameter estimates (eq (7)). Sample period: 06.23.2004-04.14.2010 (1467 observations)

¹⁸This is only true for $E(Q_t) = \bar{Q} = I_n$, otherwise $(\iota' - aa' - bb') \odot \bar{Q}$ is not necessarily positive semidefinite.

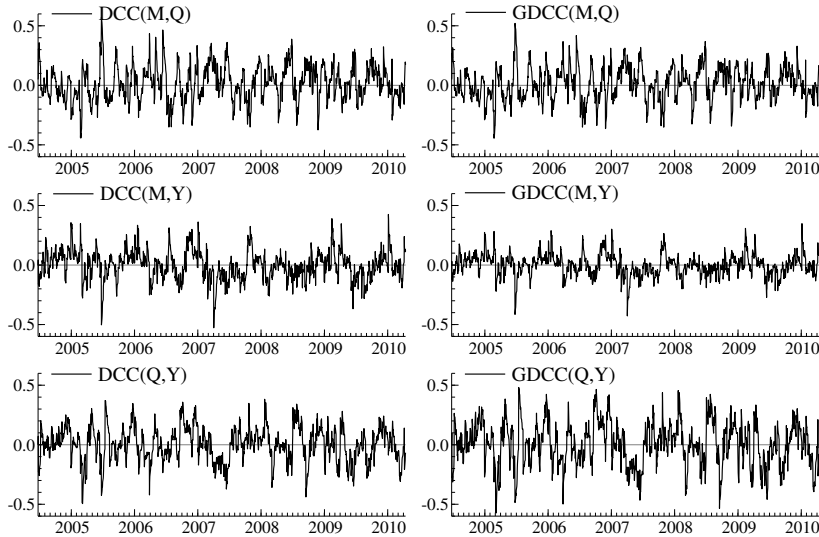


Figure 7: mDCC and mGDCC conditional correlations of u_t (month-quarter, month-year, quarter-year). $DCC(i, j)/GDCC(i, j)$ are the conditional correlation between contracts i and j estimated with the mDCC/mGDCC model.

The standardized residuals \hat{z}_t obtained after this third estimation stage¹⁹ are used for diagnostic tests. Specifically, we test for autocorrelation in the squares ($\hat{z}_t \hat{z}_t'$) using the multivariate Portmanteau statistic. The observed value for the multivariate Portmanteau statistic does not allow us to confirm the absence of autocorrelation in the squared standardized residuals for both the standard DCC and the multiplicative DCC. However, the value of the statistic is significantly reduced compared to the value obtained using VECM squared residuals ($\epsilon_t \epsilon_t'$). To compare multivariate volatility models in terms of in-sample fit, we look at the total log-likelihood value.²⁰ The estimated log-likelihood of the multiplicative DCC ($\hat{l} = -1961.8$) is higher than the one of the standard DCC model ($\hat{l} = -2040.9$) and the best model, according to this criterion, is the multiplicative GDCC model where conditional variances are adjusted for congestion and seasonality ($\hat{l} = -1904.5$).

7 Short-term forecasts of Phelix futures covariance matrix

Our ultimate objective in this paper is to provide joint forecasts of the volatility matrix of Phelix baseload futures. We give priority to short run forecasting where the future long-term covariance matrix is approximated by a constant. Let us mention however the possibility to forecast the nonparametrically estimated covariance matrix by a Taylor series expansion as discussed in Hafner

¹⁹ $\hat{z}_t = \hat{H}_t^{-1/2} \epsilon_t$.

²⁰The total estimated log-likelihood is $\hat{l} = -0.5 \left[\sum_{t=1}^T \log(|\hat{H}_t|) + \epsilon_t' \hat{H}_t^{-1} \epsilon_t \right]$.

and Linton (2010). For short-term forecasts it seems relevant to overlook the evolution of the long-term covariance matrix and to replace it by a constant. We could simply take the estimated unconditional matrix on the last day of the estimation sample. But this procedure is problematic in the case of nonparametric estimation for two reasons: it is known that the nonparametric smoothing method is less accurate near the boundary of the observation interval and for forecasting, the level of the unconditional covariance on the last day is not consistent since the estimate is obtained using out-of-sample data. A solution is then to use one-sided kernels. We follow an alternative method where the future unconditional covariance matrix is approximated replacing the Gaussian kernel by a bounded one (e.g. Epanechnikov kernel) and stopping the regression $h \times T$ days before the out-of-sample limit,²¹ ensuring the nonparametric regression to be exclusively based on in-sample data.

As for the conditional part, due to the non-linearity of the DCC process, there is no direct solution for forecasting correlations over longer horizons than one day. Engle and Sheppard (2001) discuss two approximation methods to generate multi-step ahead forecasts. We limit the scope of this paper to one-step forecasts for which there exists a straightforward solution. The one-day ahead forecast of the covariance matrix is given by

$$\hat{H}_{t+1} = \mathbb{E}(H_{t+1}|\mathcal{F}_t) \simeq \hat{\Sigma}(t/T)^{1/2} \mathbb{E}(G_{t+1}|\mathcal{F}_t) \hat{\Sigma}(t/T)^{1/2}$$

where $\hat{\Sigma}(t/T) \approx \hat{\Sigma}(t/T - h)$ and regression weights are derived using Epanechnikov kernels.

We compute rolling one-day ahead forecasts over H days for the variances and covariances of baseload futures according to two different procedures. In the first method, forecasts are based on recursive estimation where one day is added to the estimation sample each day so that parameters are updated daily. In the second, the estimation sample and the parameters are fixed and forecasts are computed each day based on the exogenous variables and on the forecasted values of the covariance matrix and VECM residuals obtained the day before.

Rolling forecasts (black lines) based on recursive estimation over six months (130 trading days) from 04.15.2010 until 10.15.2010 are illustrated in Figure 8 for one model. Because of the lack of intraday data for futures prices we cannot compare the forecasts with realized variances and covariances. Instead of realized data, we take the squares (colorful lines) and cross-products (grey lines) of VECM residuals as proxies for variances and covariances respectively.

²¹with $h = 0.09$, the optimal bandwidth for the Epanechnikov kernel and T , the in-sample size.

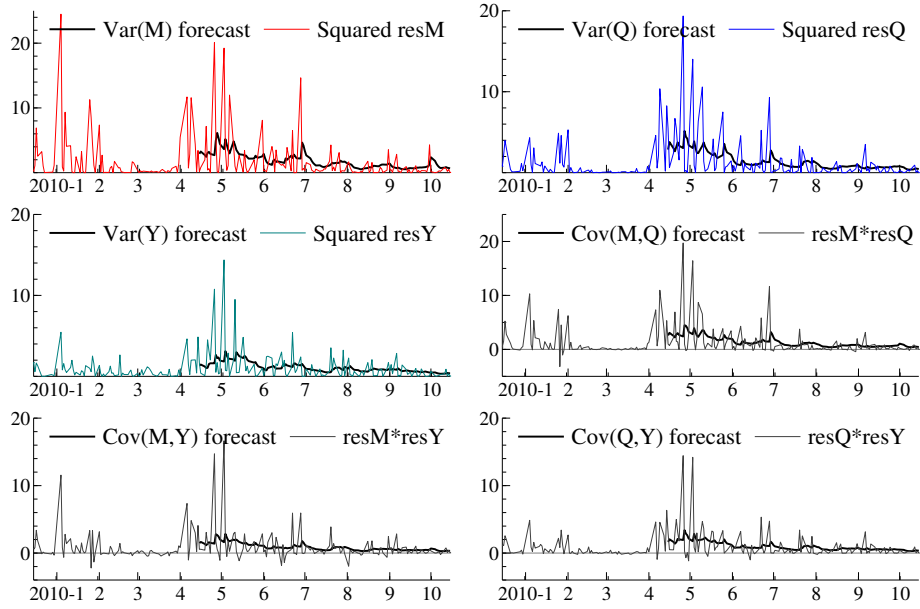


Figure 8: 130 day rolling forecasts (seasonal congestion mGDCC, recursive estimation). The one-day ahead variance forecasts of contract i is $Var(i)$ forecast = $\hat{H}_{ii,t+1}$. The one-day ahead covariance forecasts of contracts i and j is $Cov(i, j)$ forecast = $\hat{H}_{ij,t+1}$ for $i \neq j$. $res(i)$ are VECM residuals.

We compare different specifications for the covariance matrix of Phelix futures in terms of mean squared forecasting error (MSE) in the next tables. Tables 7 and 8 report the performance of rolling one-day ahead forecasts over 130 days using recursive and fixed sample estimation, respectively. The obtained forecasts of variances and covariances are based on one-day ahead forecasts for the VECM residuals using the same fixed estimation sample. For each procedure, the multiplicative generalized DCC model with congestion and seasonality variables (sc-mGDCC) is the best performing model. The largest improvement comes with the multiplicative DCC model (mDCC) compared to the standard DCC (DCC) that ignores slowly evolving trends in volatilities and co-volatilities. The multiplicative generalized DCC model (mGDCC) and the seasonal and congestion effects in volatilities only bring some small improvements. As expected, only the forecasts of short-term maturity products (month and quarter futures) are improved when incorporating a seasonal effect (s-mGDCC). The congestion model for volatilities seems also to be more useful for short-term products for which we observe the largest spikes in the conditional variances and covariances. In this case, the exogenous variables are able to capture, to some extent, the spikes that are induced by transmission constraints so that the congestion model would be favored during more hectic times.

Model	Var(M)	Var(Q)	Var(Y)	Cov(M,Q)	Cov(M,Y)	Cov(Q,Y)	Total
DCC	10.672	7.048	3.667	7.738	4.935	4.208	38.267
mDCC	9.646	6.374	3.518	7.101	4.685	3.975	35.300
mGDCC	9.588	6.392	3.534	7.078	4.670	3.999	35.261
s-mGDCC	9.381	6.417	3.548	7.064	4.670	4.022	35.102
sc-mGDCC	9.371	6.396	3.544	7.051	4.666	4.012	35.038

Table 7: MSE ($H = 130$, recursive estimation)

Model	Var(M)	Var(Q)	Var(Y)	Cov(M,Q)	Cov(M,Y)	Cov(Q,Y)	Total
DCC	10.107	6.691	3.657	7.403	4.865	4.129	36.852
mDCC	9.552	6.307	3.496	7.011	4.637	3.932	34.935
mGDCC	9.520	6.317	3.502	6.995	4.619	3.945	34.897
s-mGDCC	9.257	6.306	3.511	6.955	4.616	3.956	34.601
sc-mGDCC	9.230	6.305	3.517	6.944	4.616	3.957	34.569

Table 8: MSE ($H = 130$, fixed estimation sample)

8 Conclusion

We have presented a new multiplicative model for the multivariate volatility of Phelix baseload futures where the unconditional volatilities and correlations are allowed to change smoothly over time. The evolution of the unconditional component is explained by long-term factors observed in power markets. We also introduce a seasonal congestion model accounting for transmission shocks and seasonality in the conditional volatility of futures contracts. It is shown that futures respond to congestion with different markets according to their maturity. An augmented multiplicative DCC model that allows for component-specific dynamics is applied for modeling the conditional correlations of electricity futures. Specifically, a higher persistence and amplified movements are found for the conditional correlation of long-term contracts. Finally, rolling one-step ahead forecasts are derived and a higher forecasting performance is achieved with the multiplicative DCC model compared to the standard DCC model that ignores the changes in unconditional volatilities and correlations. More generally, the multiplicative DCC model could respond to the modeling needs for other markets that are subject to changing long-term trends.

References

- Aielli, G. (2009). Dynamic conditional correlations: on properties and estimation. Technical report, Department of Statistics, University of Florence.
- Bauwens, L., S. Laurent, and J. Rombouts (2006). Multivariate GARCH models: a survey. *Journal of Applied Econometrics* 21, 79–109.
- Bauwens, L., A. Preminger, and J. Rombouts (2010). Theory and inference for a Markov-switching GARCH model. *Econometrics Journal* 13, 218–244.
- Bauwens, L. and G. Storti (2009). A component GARCH model with time varying weights. *Studies in Nonlinear Dynamics & Econometrics* 13(2), Article 1.
- Billio, M. and M. Caporin (2009). A generalized dynamic conditional correlation model for portfolio risk evaluation. *Mathematics and Computers in Simulation* 19(8), 2566–2578.
- Borovkova, S. and H. Geman (2006). Analysis and modeling of electricity futures prices. *Studies in Nonlinear Dynamics & Econometrics* 10(3), Article 6.
- Bosco, B., L. Parisio, M. Pelagatti, and F. Baldi (2010). Long-run relations in European electricity prices. *Journal of Applied Econometrics* 25, 805–832.
- Cappiello, L., R. Engle, and K. Sheppard (2006). Asymmetric dynamics in the correlations of global equity and bond returns. *Journal of Financial Econometrics* 4, 537–372.
- Carnero, A., S. Koopman, and M. Ooms (2007). Periodic heteroskedastic RegARFIMA models for daily electricity spot prices. *Journal of the American Statistical Association* 102(477), 16–27.
- Colacito, R., R. Engle, and E. Ghysels (2009). A component model for dynamic correlations. NYU Working Paper No. FIN-08-039.
- De Jong, C. and S. Schneider (2009). Cointegration between gas and power spot prices. *The Journal of Energy Markets* 2(3), 27–46.
- Engle, R. (2002). Dynamic conditional correlation: a simple class of multivariate generalized autoregressive conditional heteroskedasticity models. *Journal of Business and Economic Statistics* 20(3), 339–350.
- Engle, R. and G. Lee (1999). A long-run and short-run component model for stock return volatility. In R. F. Engle and H. White (Eds.), *Cointegration, Causality, and Forecasting: A Festschrift in Honour of Clive W. J. Granger*, Chapter 20, pp. 475–497. Oxford University Press.
- Engle, R. and J. Rangel (2008). The spline-GARCH model for low-frequency volatility and its global macroeconomic causes. *Review of Financial Studies* 21 (3), 1187–1222.
- Engle, R. and K. Sheppard (2001). Theoretical and empirical properties of dynamic conditional correlation multivariate GARCH. NBER Working Paper No. 8554.
- Geman, H. (2005). *Commodities and commodity derivatives, modeling and pricing for agriculturals, metals and energy*. Wiley Finance.

- Glosten, L., R. Jagannathan, and D. Runkle (1993). On the relation between the expected value and the volatility of the nominal excess return on stocks. *The Journal of Finance* 48(5), 1779–1801.
- Haas, M., S. Mittnik, and M. Paolella (2004a). Mixed normal conditional heteroskedasticity. *Journal of Financial Econometrics* 2:2, 211–250.
- Haas, M., S. Mittnik, and M. Paolella (2004b). A new approach to Markov-switching GARCH models. *Journal of Financial Econometrics* 2:4, 493–530.
- Hafner, C. and P. Franses (2009). A generalized dynamic conditional correlation model: simulation and application to many assets. *Econometric Reviews* 28(6), 612–631.
- Hafner, C. and O. Linton (2010). Efficient estimation of a multivariate multiplicative volatility model. *Journal of Econometrics* 159(1), 55–73.
- Haldrup, N. and M. Nielsen (2006). Directional congestion and regime switching in a long memory model for electricity prices. *Studies in Nonlinear Dynamics & Econometrics* 10(3), Article 1.
- Härdle, W. (1990). *Applied Nonparametric Regression*. Cambridge University Press.
- Johansen, S. (1991). Estimation and hypothesis testing of cointegration vectors in Gaussian vector autoregressive models. *Econometrica* 59, 1551–1580.
- Knittel, C. and M. Roberts (2005). An empirical examination of restructured electricity prices. *Energy Economics* 27, 791–817.
- Pelletier, D. (2006). Regime switching for dynamic correlations. *Journal of Econometrics* 131, 445–473.
- Pilipovic, D. (2007). *Energy risk, valuing and managing energy derivatives. 2nd edition*. McGraw-Hill.
- Rangel, J. and R. Engle (2009). The factor-spline-GARCH model for high and low frequency correlations. Banco de Mexico Working Paper No. 2009-03.
- Samuelson, P. (1965). Proof that properly anticipated prices fluctuate randomly. *Industrial Management Review* 6, 41–49.
- Silvennoinen, A. and T. Teräsvirta (2005). Modeling conditional correlations of asset returns: a smooth transition approach. SSE/EFI Working Paper Series in Economics and Finance No. 577.
- Silvennoinen, A. and T. Teräsvirta (2009). Multivariate GARCH models. *Handbook of Financial Time Series Part 1*, 201–229.
- Wilkens, S. and J. Wimschulte (2007). The pricing of electricity futures: evidence from the European Energy Exchange. *The Journal of Futures Markets* 27 (4), 387–410.